CLINICAL SCIENCE

Predicting dysthyroid optic neuropathy using computed tomography volumetric analyses of orbital structures

Allan C. Pieroni Gonçalves,[I] Lucas Nunes Silva,[II] Eloísa M. M. S. Gebrim,[II] Suzana Matayoshi,[I] Mário Luiz Ribeiro Monteiro[I]

[I] Faculdade de Medicina da Universidade de São Paulo, Division of Ophthalmology, São Paulo/SP, Brazil. [II] Faculdade de Medicina da Universidade de São Paulo, Department of Radiology, São Paulo/SP, Brazil.

OBJECTIVE: To evaluate the ability of orbital apex crowding volume measurements calculated with multidetector-computed tomography to detect dysthyroid optic neuropathy.

METHODS: Ninety-three patients with Graves' orbitopathy were studied prospectively. All of the patients underwent a complete neuro-ophthalmic examination and computed tomography scanning. Volumetric measurements were calculated from axial and coronal contiguous sections using a dedicated workstation. Orbital fat and muscle volume were estimated on the basis of their attenuation values (in Hounsfield units) using measurements from the anterior orbital rim to the optic foramen. Two indexes of orbital muscle crowding were calculated: i) the volumetric crowding index, which is the ratio between soft tissue (mainly extraocular muscles) and orbital fat volume and is based on axial scans of the entire orbit; and ii) the volumetric orbital apex crowding index, which is the ratio between the extraocular muscles and orbital fat volume and is based on coronal scans of the orbital apex. Two groups of orbits (with and without dysthyroid optic neuropathy) were compared.

RESULTS: One hundred and two orbits of 61 patients with Graves' orbitopathy met the inclusion criteria and were analyzed. Forty-one orbits were diagnosed with Graves' orbitopathy, and 61 orbits did not have optic neuropathy. The two groups of orbits differed significantly with regard to both of the volumetric indexes ($p<0.001$). Although both indexes had good discrimination ability, the volumetric orbital apex crowding index yielded the best results with 92% sensitivity, 86% specificity, 81%/94% positive/negative predictive value and 88% accuracy at a cutoff of 4.14.

CONCLUSION: This study found that the orbital volumetric crowding index was a more effective predictor of dysthyroid optic neuropathy than previously described computed tomography indexes were.

KEYWORDS: Dysthyroid optic neuropathy; Multidetector computed tomography; Graves' orbitopathy; Volume CT.

INTRODUCTION

Graves' orbitopathy (GO) is the most common extrathyroid manifestation of Graves' disease (GD). It occurs before, during, or after the onset of hyperthyroidism and, less frequently, in euthyroid or hypothyroid patients. The course of GO can be divided into active (congestive) and inactive (fibrotic) phases. Tissue expansion occurs within the relatively fixed volume imposed by the bony orbit and results in inflammation, the accumulation of hydrophilic glycosaminoglycans and increased fat content (1). Clinical signs include proptosis, congestive signs, strabismus, and dysthyroid optic neuropathy (DON) (2-5).

DON is the most significant complication of GO. It affects 3.4 to 8% of GO patients (6-9) and requires prompt treatment to avoid permanent visual loss. Almost all instances of DON result from optic nerve compression at the orbital apex by enlarged extraocular muscles. The diagnosis of DON includes the following clinical features: decreased visual acuity (VA), abnormal visual fields (VF), impaired color and brightness perception, delayed visual evoked potentials, afferent pupillary defects and edema or atrophy of the optic nerve head (6). Unfortunately, some of these tests require the full cooperation of an alert and motivated patient and often render false positive results, particularly in patients with congestive GO. Furthermore, alternative causes of visual impairment secondary to GO,

Volumetric CT analyses in dysthyroid optic neuropathy
Gonçalves ACP et al.

CLINICS 2012;67(8):891-896

such as exposure keratopathy or secondary glaucoma, and coincidental conditions, such as amblyopia or cataracts, may also contribute to the considerable difficulty of detecting DON (10). Because diagnosing DON can be clinically difficult and because its prognosis improves significantly with early diagnosis and treatment, it is important to design objective tests that can identify patients at risk for developing DON (11).

Computed tomography (CT) is the most frequently used imaging modality in patients with GO because of its capacity to visualize bone and soft tissue in the orbit. Previous studies have shown that a number of CT scan parameters can help to detect and facilitate the diagnosis of DON, primarily those parameters based on the detection of orbital apical crowding by enlarged extraocular muscles (4-6,12-16). Crowding has been successfully estimated with CT parameters, such as linear measurements of extraocular muscles (4,5,11,13), the subjective assessment of apical crowding (on single coronal images) (4,11,16,17) and measurements of the area (11) and volume (18,19) of the orbital muscles.

Although linear and area measurements have proven to be helpful in the diagnosis of DON, the assessment of orbital apex crowding using volumetric estimates of structures could potentially improve the ability to detect and diagnose DON. In fact, Feldon et al. (2,18) used volumetric estimates of orbital contents to investigate the risk of developing DON in GO patients; however, those authors' measurements required cumbersome manual calculations of the orbital muscles and other orbital structures. The recent introduction of multidetector-row computed tomography (MDCT) has resulted in shorter scanning times and higher resolution and has made it possible to reformat images from any plane, making orbital measurements easier to take and more precise. Using software for three-dimension orbital structure analysis, volumetric measurements can be easily calculated at a workstation (20).

The purpose of this study was therefore to quantify muscle crowding and use it to test the ability of two volumetric indexes of muscle crowding based on volume measurements obtained with multidetector-computed tomography to predict DON in the orbits of GO patients.

PATIENTS AND METHODS

The study followed the tenets of the Declaration of Helsinki and was approved by an institutional ethics committee. Ninety-three new patients with GO who were admitted to the orbit service of a tertiary referral eye center during the five-year study period were prospectively included. GO was diagnosed in accordance with previously established criteria (21). All of the patients underwent a complete neuro-ophthalmic examination, including best-corrected VA, applanation tonometry, pupillary reactions, extraocular motility evaluation, slit lamp examination, soft tissue and eyelid inflammation evaluation, lid fissure measurement, Hertel exophthalmometry, fundoscopy, and VF evaluation.

VF testing was performed using manual perimetry and standard automated perimetry (SAP). Manual VF testing was performed using the Goldmann perimeter (GP) (Haag-Streit AG, Bern, Switzerland). SAP was performed with a Humphrey Field Analyzer 750 (Zeiss-Humphrey, Dublin, CA) using the 24-2 SITA-Standard strategy. The patients'

appropriate near correction was used. To qualify as an abnormal VF on SAP, three adjacent abnormal points at the $p<0.05$ level or two adjacent points with one abnormal point at the $p<0.01$ level on the pattern deviation plot were required (22). Exclusion criteria included the following: age under 20 years, inability to cooperate with VF testing, spherical refraction over ± 5 D, cylinder correction over ± 3 D and unreliable VF test results. An unreliable Humphrey VF test was defined as one with more than 25% fixation losses, false-positive or false-negative responses. Patients with clinical signs of glaucomatous optic neuropathy, optic disc anomaly, optic media opacities, previous orbital or strabismus surgery, and other types of neuropathies were also excluded.

All patients were scanned with a 16-slice MDCT scanner (Brilliance 16; Philips Medical Systems, Nederland B.V., The Netherlands) without the use of sedation or intravenous contrast. The CT scans were obtained using contiguous axial slices, with the patient's head positioned parallel to the Frankfurt plane. The patients were instructed to keep their eyes closed and steady in the primary gaze position. The scanning parameters were as follows: 120 Kv, 200 mAs, 16x0.75 mm detector configuration, 1.5 mm slice thickness and 0.7 mm slice increment. The images were postprocessed at a dedicated workstation and read by a single head-and-neck radiologist (L.N.S) who was blinded to the patients' clinical condition.
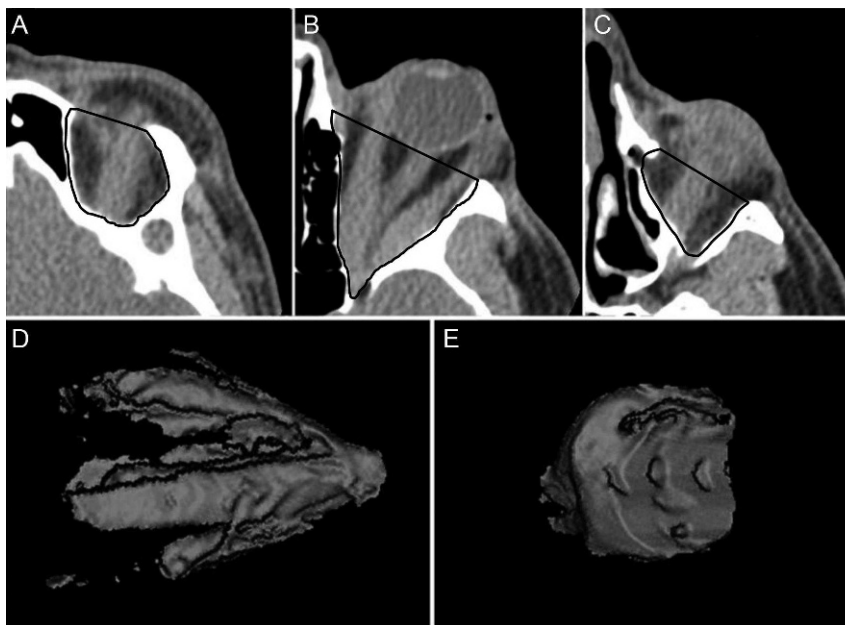
Two volumetric indexes were calculated, one based on axial scans of the entire orbit content (up to the orbital rim) and one based on coronal scans of the orbital content from the midpoint of the orbital segment of the optic nerve to the orbital entrance of the optic canal.

Volume measurements of the entire orbit from axial scans

To calculate volumes for the whole orbital content, contiguous axial scans were analyzed. The different tissues were color-coded according to their attenuation in Hounsfield units (HU). Tissue HU thresholds were defined using different window levels (WL) and window widths (WW) to separate the soft tissue (which mainly includes muscles, nerves and vessels) from other orbital tissues (mainly fatty content). Orbital soft tissue thresholds were set at 40/100 HU (WL/WW), and the fat tissue threshold was set at -160/230 HU (WL/WW). For the tissue volume measurements, each axial slice was traced along the bony orbit limits. The anterior boundary of the orbit was delineated by a straight line connecting the lateral and the medial orbital rim (Figure 1). The marking began at the topmost axial slice containing the orbit and continued downwards, slice by slice, until all of the orbit content was included. The volume of the muscles (including vessels and nerves), soft tissues and fat within the marked space was then estimated with the software (Figure 1). The volumetric orbital muscle crowding index (VCI) was calculated as the ratio between the soft tissue volume and the fat tissue volume.

Volume measurements of the orbital apex from coronal scans

One-millimeter coronal CT slabs were reformatted from contiguous axial slices of the orbit, which includes the space between the interzygomatic line and the orbital apex (Figure 2). The orbital volume was calculated from the

CLINICS 2012;67(8):891-896

Volumetric CT analyses in dysthyroid optic neuropathy
Gonçalves ACP et al.

Figure 1 - A, B and C. Examples of the area outlined on 3 axial slices of computed tomography scans, from which measurements were obtained. Representation of the soft tissue (mostly muscles; D) and orbital fat (E) volumes based on measurements of the sequential axial slices.

posterior portion of the orbit, which encompasses the tissues within a point in the optic nerve halfway between the globe and the orbital apex and up to the entrance of the optic canal. The fat and soft tissues were color-coded with the same settings used for the axial measurements. For each of the preset coronal planes, a region of interest was traced around the orbital bone rim (Figure 2). The software automatically calculated the total volume of fat and soft tissue in that region (Figure 2). The ratio of the soft tissue volume to the fat volume (using volume measures taken at the apex) was calculated to determine the volumetric orbital apex crowding index (VACI).
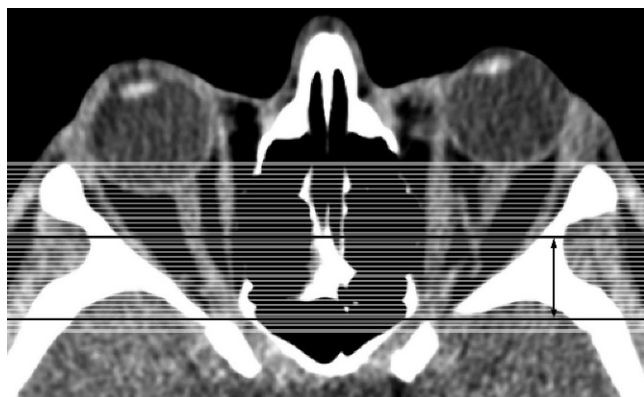
The same reader repeated the measurements for 26 randomly selected orbits (13 with DON) approximately

Figure 2 - Percentage difference from rest to ventilatory anaerobic threshold (rest/VAT), rest to respiratory compensation point (rest/RCP) and rest to peak of exercise (rest/Peak) in patients with coronary artery disease subjected to continuous exercise training (panel A) and interval exercise training (panel B). VAT = ventilatory anaerobic threshold; RCP = respiratory compensation point. * $p < 0.05$ vs. post-intervention.

eight months after the first measurements. On a different occasion, the same group of orbits was independently measured by a senior radiologist (E.M.M.S.G.). Both readers were blinded to the presence or absence of DON.

GO patients' eyes for which visual function data clearly indicated the presence or absence of active DON were considered eligible for the study. The criteria used to diagnose DON included the following: 1) The presence of a confirmed VF defect on SAP or GP associated or not with diminished best-corrected VA and not caused by changes in transparency and 2) in unilateral and asymmetric cases, the presence of a relative pupillary defect. When the best-corrected VA was normal and VF abnormalities were present on SAP, a repeat examination using SAP or GP was performed to rule out false-positive responses. Therefore, only eyes with confirmed VF defects were included in the analysis. Eyes with normal VA and nonreproducible VF abnormalities on repeat examinations were excluded. Patients with ocular or optic nerve diseases that could interfere with the diagnosis of DON were also excluded. All patients with DON had active disease, visual disturbance within three months of the onset of the disease and clinical signs of orbital congestive disease. Patients from the group without DON had a history of orbital disease ranging from two months to four years. The findings for the two groups were compared.

Statistical analysis

Descriptive statistics included the mean values $\pm$ SD for normally distributed variables. Receiver operating characteristic (ROC) curves were used to describe the ability of the VCI and the VACI to discriminate between orbits with and without DON. For each parameter, sensitivities at the fixed specificities of 80% and 95% were calculated. Sensitivity, specificity, likelihood ratio, and accuracy were calculated for the best cutoff values of VCI and VACI. The intraclass

Volumetric CT analyses in dysthyroid optic neuropathy
Gonçalves ACP et al.

CLINICS 2012;67(8):891-896

Table 1 - Means ± standard deviation of the axial volumetric orbital crowding index (VCI) and the coronal volumetric orbital apex crowding index (VACI) in the orbits of patients with Graves' orbitopathy (GO) with or without dysthyroid optic neuropathy (DON).

Parameter	Orbits with DON n = 41	Orbits without DON n = 61	p-value*
Mean ± SD VCI	1.84 ± 1.02	0.83 ± 0.28	<0.001
95% CI	1.52–2.16	0.76–0.90	
Range	0.31–5.28	0.34–1.53	
Mean ± SD VACI	21.35 ± 21.09	2.82 ± 2.28	<0.001
95% CI	14.69–28.01	2.24–3.40	
Range	1.03–86.52	0.59–10.97	

*Student's t-test. Significant values are in italics. CI = confidence interval.

correlation coefficient (ICC) was calculated to assess the interrater and intrarater variability for the VCI and VACI measurements. A *p*-value less than 0.05 was considered statistically significant.

RESULTS

Thirty-two of the 93 patients were excluded based on theabove-described criteria. The remaining 61 patients (37 women and 24 men) had 102 orbits that were included in the study. The orbits were divided into two groups according to the presence or absence of DON. The first group included 41 orbits of 27 patients (12 women and 15 men; mean age ± SD: 53.8 ± 10.1 years) who met the diagnostic criteria for DON. Fourteen patients had bilateral DON; for those patients, both orbits were included in the study. Thirteen patients had only one orbit included in the DON group. Of these 13 patients, the contralateral eye of ten patients did not meet the DON criteria. Two patients had the contralateral eye excluded because the presence or absence of DON could not be clearly determined; in one patient, a history of central retinal artery occlusion unrelated to GO excluded the contralateral eye. The second group included 61 orbits in which DON was clearly absent from 34 patients (25 women and nine men; mean age ± SD: 42.3 ± 10.2 years). In this group, seven orbits were excluded from analysis because of the uncertainty of the DON diagnosis. Six of these patients had questionable VF abnormalities on SAP even after repeat examinations. One patient had an eye with severe deviations caused by extraocular muscle involvement, which precluded proper VF examination.

For the 41 orbits with DON, the best-corrected VA was 1.0 in 20 patients, 0.9 in seven patients, 0.8 in six patients, 0.7 in one patient, 0.6 in two patients, 0.4 in one patient, 0.5 in two patients, 0.2 in one patient, and 0.1 in one patient. Exophthalmometry measurements in the affected eyes ranged from 19 to 32 mm (mean ± SD: 25.14 ± 3.19 mm). Restrictive myopathy was present in all orbits with DON. The fundoscopic examination revealed optic disc edema in eight eyes, optic disc pallor in one and no abnormalities in the remainder. In the group without DON, the best-corrected VA was 1.0 in all eyes, and exophthalmometry findings ranged from 16.0 to 31.5 mm (mean ± SD: 23.4 ± 2.7).

Table 1 shows the mean ± SD and the ranges for the VCI and VACI. The mean VCI and VACI values were significantly higher in the orbits with DON (*p*<0.001).

Table 2 compares the two groups' areas under ROC curves for the two volumetric indexes, with confidence intervals and sensitivity at the 95% and 80% specificity rates. The area under the ROC curve was 0.86 for the VCI and 0.92 for the VACI. Cutoff values were determined for the two indexes to calculate their sensitivity and specificity for differentiating orbits with and without DON. The best sensitivity/specificity ratio was achieved with a VACI cutoff of 4.14 (sensitivity: 90%, specificity: 87%, likelihood ratio: 6.9, accuracy for detecting DON: 88%; Table 2).
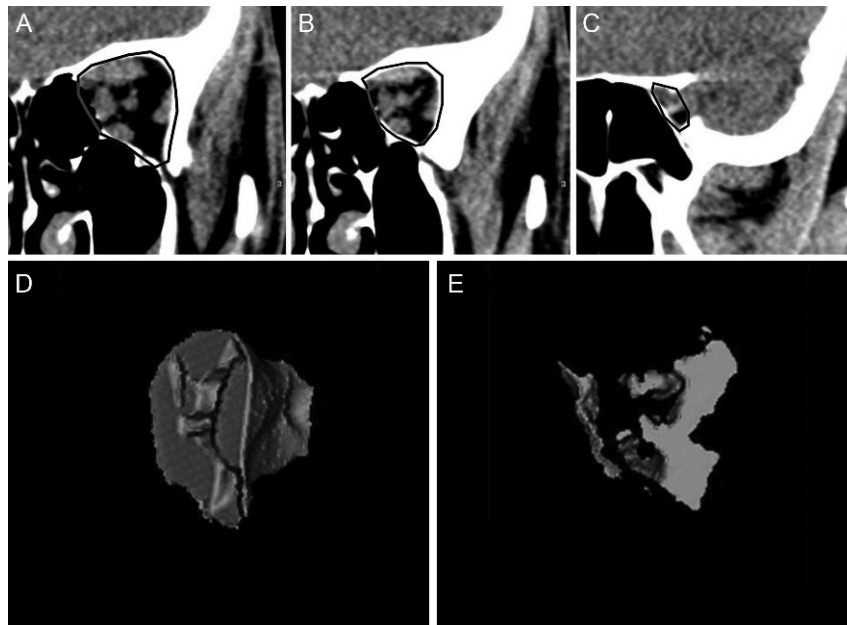
The ICCs for the VCI and VACI as determined by the second observer were 0.90 and 0.91, respectively (*p*<0.001), indicating an excellent interobserver variability. Corresponding values for repeated measurements by the same observer were 0.90 and 0.89, indicating excellent intraobserver variability (*p*<0.001).

DISCUSSION

GO can be an insidious disease, and DON is a significant complication that requires prompt diagnosis and treatment to prevent permanent visual damage. Although research has suggested that DON may be caused by inflammatory and vascular mechanisms, the most widely accepted theory for DON development is direct compression of the optic nerve by enlarged extra ocular muscles at the orbital apex (3,6,23,24). The diagnosis of DON depends mainly on clinical features based on visual function assessment, afferent pupillary defect and fundoscopic abnormalities. Nevertheless, DON is often subclinical and in many cases, it is difficult to diagnose because of confounding signs and symptoms. Furthermore, patients with severe orbitopathy tend to have more congestive and oculomotor symptoms, which may outweigh or mask subtle visual deterioration (6). Therefore, the development of imaging techniques that facilitate the diagnosis of DON is highly desirable.

Table 2 - Area under the receiver operating characteristics curves (AUC) and sensitivities at fixed specificities for the volumetric crowding index (VCI) and the volumetric apical crowding index (VACI). Sensitivity, specificity, likelihood ratio (LR) and accuracy are presented for the best cutoff values of VCI and VACI.

Parameter	AUC (SE)	Sensitivity/specificity		Cutoff value	Sensitivity/specificity at cutoff value	LR (95% CI)	Accuracy (95% CI)
		Specificity ≥ 95%	Specificity ≥ 80%				
VCI	0.86 (0.04)	56/95	71/80	1.08	71%/80%	3.6 (2.1-6.2)	76% (67%-85%)
VACI	0.92 (0.31)	66/95	93/80	4.14	90%/87%	6.9 (3.9-10.8)	88% (80%-93%)

CLINICS 2012;67(8):891-896

Volumetric CT analyses in dysthyroid optic neuropathy
Gonçalves ACP et al.

Figure 3 - A, B and C. Examples of the area outlined on 3 coronal slices of computed tomography scans, from which measurements were obtained. Representation of the soft tissue (mostly muscles) (D) and orbital fat (E) apical volumes based on sequential coronal orbital slices.

Previous CT studies have demonstrated a direct correlation between orbital apex crowding by enlarged extraocular muscles and the development of DON (6,12,13,18,24,25). Recent studies also suggest that bony orbit anatomy may play an important role in the development of DON because narrow orbits are more susceptible to apex crowding (11). In addition, other CT features (such as intracranial fat prolapse, lacrimal gland displacement, exophthalmos severity and superior ophthalmic vein dilatation) have been proposed but have not been confirmed as useful for detecting DON (4,6,11,17,24,26).

Because the presence of apical crowding on CT imaging is strongly correlated with DON in GO, several authors have proposed indexes for detecting DON. Barret et al. (13) calculated a linear muscle index from CT images and found it to be reproducible and reasonably efficient for detecting DON. In a previous study, we investigated the sensitivity and specificity of this muscle index calculation with MDCT and found the best combination (79% sensitivity and 72% specificity) at a muscle index of 60% (5). Nugent et al. (14) proposed a categorical scale for apical crowding, which was later reproduced by many other authors (4,11,16,17). Using this method, Nugent et al. (14) found severe apical orbital crowding in 12 out of 18 orbits with DON, but only in 16 out of 124 orbits without DON. While it seems clear that crowding scores are useful for detecting DON, the accurate use of the scores is difficult because the authors of these studies did not provide clear definitions of the positions along the orbit where the coronal plan was used to determine their scores.

In our study, we attempted to improve on existing CT indexes with a volumetric quantification of orbital crowding. In previous studies, extraocular muscle volume estimates were useful for detecting DON, but the manual quantitative analysis of the extraocular measurements was time-consuming and complex (12,18,25). In our study, orbital structures could be precisely reformatted using an MDCT scanner, and the measurement of the orbital structures with the volumetric analysis software was straightforward. The technology has mainly been used in studies to estimate the increase in orbital fat, the effect of orbital radiotherapy or the effect of orbital decompression on orbital structures. However, to our knowledge, no previous study has evaluated the technology's ability to predict DON (19,27-31). According to published guidelines for the radiologic measurement of tissue volumes in GO patients, there is currently no consensus on how to measure orbital fat and extraocular muscle volume (32). To obtain volume measurements, we used a computer-assisted algorithm based on the density of soft tissue and orbital fat. We then calculated the following two volumetric indexes: the VCI, which is the ratio of the extraocular muscle volume to the orbital fat volume and is based on axial scans of the entire orbit; and the VACI, which is the ratio of the extraocular muscle volume to the orbital fat volume and is based on coronal scans of the orbital apex. The indexes appeared to be reliable and reproducible, as suggested by the high ICC values found in this study.

In our study, all patients were carefully and prospectively evaluated for the presence or absence of DON, and a large number of orbits with optic neuropathy were included. Both indexes were efficient at differentiating patients with DON from patients without DON. The VACI, which evaluates the orbital apex, was particularly effective; it achieved a sensitivity of 90% and a specificity of 87% at a cutoff of 4.14, whereas the VCI achieved only 71% sensitivity and 80% specificity at a cutoff of 1.08. These findings indicate that volumetric orbital crowding measurements are better at detecting DON in patients with GO when they are restricted to the orbital apex.

Our analysis of the performance of the VACI indicates a significant improvement over previous indexes in identifying patients with DON. The VACI was more efficient than

Volumetric CT analyses in dysthyroid optic neuropathy
Gonçalves ACP et al.

CLINICS 2012;67(8):891-896

both the Nugent scale, which was evaluated in several previous studies (4,14,16,17), and the linear muscle index described by Barret et al. (13). The latter suggested that an index of 67% or greater would have a diagnostic sensitivity of 67% for detecting DON (13). In a previous study that investigated the sensitivity and specificity of this muscle index using MDCT, the best sensitivity/specificity combination (79%/72%) was observed at a muscle index of 60% (5). This is clearly inferior to the performance of the indexes tested in the current study.

In conclusion, our study tested the value of two volumetric indexes for assessing the degree of apical crowding, one based on measurements of the entire orbit and one based on measurements of the orbital apex only. Both indexes were found to be efficient at predicting DON, although the latter index was more effective. Further studies are necessary to validate our findings.

ACKNOWLEDGMENTS

AUTHOR CONTRIBUTIONS

Gonçalves AC contributed to the project design, data collection, data management, and writing the manuscript. Silva LN designed the project and collected data. Gebrim EM designed the project, collected data and revised the manuscript. Matayoshi S designed the project and revised the manuscript. Monteiro ML designed the project, analyzed data, and wrote and revised the manuscript.

REFERENCES

1. Naik VM, Naik MN, Goldberg RA, Smith TJ, Douglas RS. Immunopathogenesis of thyroid eye disease: emerging paradigms. Surv Ophthalmol. 2010;55(3):215-26, http://dx.doi.org/10.1016/j.survophthal.2009.06.009.
2. Hallin ES, Feldon SE. Graves' ophthalmopathy: II. Correlation of clinical signs with measures derived from computed tomography. Br J Ophthalmol. 1988;72(9):678-82.
3. Monteiro MLR, Moritz RBS, Angotti-Neto H, Moritz R, Benabou J. Color Doppler imaging of the superior ophthalmic vein in patients with Graves' orbitopathy before and after treatment of congestive disease. Clinics. 2011;66(6):1329-34.
4. Giaconi JA, Kazim M, Rho T, Pfaff C. CT scan evidence of dysthyroid optic neuropathy. Ophthal Plast Reconstr Surg. 2002;18(3):177-82.
5. Monteiro ML, Goncalves AC, Silva CT, Moura JP, Ribeiro CS, Gebrim EM. Diagnostic ability of Barrett's index to detect dysthyroid optic neuropathy using multidetector computed tomography. Clinics. 2008;63(3):301-6, http://dx.doi.org/10.1590/S1807-59322008000300003.
6. Neigel JM, Rootman J, Belkin RI, Nugent RA, Drance SM, Beattie CW, et al. Dysthyroid optic neuropathy. The crowded orbital apex syndrome. Ophthalmology. 1988;95(11):1515-21.
7. Bartley GB. The epidemiologic characteristics and clinical course of ophthalmopathy associated with autoimmune thyroid disease in Olmsted County, Minnesota. Trans Am Ophthalmol Soc. 1994;92:477-588.
8. Ben Simon GJ, Syed HM, Douglas R, Schwartz R, Goldberg RA, McCann JD. Clinical manifestations and treatment outcome of optic neuropathy in thyroid-related orbitopathy. Ophthalmic Surg Lasers Imaging. 2006;37(4):284-90.
9. Monteiro ML, Portes AL, Moura FC, Regensteiner DB. Using frequency-doubling perimetry to detect optic neuropathy in patients with Graves' orbitopathy. Jpn J Ophthalmol. 2008;52(6):475-82, http://dx.doi.org/10.1007/s10384-008-0579-x.
10. Dayan CM, Dayan MR. Dysthyroid optic neuropathy: a clinical diagnosis or a definable entity? Br J Ophthalmol. 2007;91(4):409-10, http://dx.doi.org/10.1136/bjo.2006.110932.
11. Chan LL, Tan HE, Fook-Chong S, Teo TH, Lim LH, Seah LL. Graves ophthalmopathy: the bony orbit in optic neuropathy, its apical angular capacity, and impact on prediction of risk. AJNR Am J Neuroradiol. 2009;30(3):597-602, http://dx.doi.org/10.3174/ajnr.A1413.
12. Feldon SE, Muramatsu S, Weiner JM. Clinical classification of Graves' ophthalmopathy. Identification of risk factors for optic neuropathy. Arch Ophthalmol. 1984;102(10):1469-72.
13. Barrett L, Glatt HJ, Burde RM, Gado MH. Optic nerve dysfunction in thyroid eye disease: CT. Radiology. 1988;167(2):503-7.
14. Nugent RA, Belkin RI, Neigel JM, Rootman J, Robertson WD, Spinelli J, et al. Graves orbitopathy: correlation of CT and clinical findings. Radiology. 1990;177(3):675-82.
15. Ozgen A, Alp MN, Ariyurek M, Tutuncu NB, Can I, Gunalp I. Quantitative CT of the orbit in Graves' disease. Br J Radiol. 1999;72(860):757-62.
16. McKeag D, Lane C, Lazarus JH, Baldeschi L, Boboridis K, Dickinson AJ, et al. Clinical features of dysthyroid optic neuropathy: a European Group on Graves' Orbitopathy (EUGOGO) survey. Br J Ophthalmol. 2007;91(4):455-8, http://dx.doi.org/10.1136/bjo.2006.094607.
17. Birchall D, Goodall KL, Noble JL, Jackson A. Graves ophthalmopathy: intracranial fat prolapse on CT images as an indicator of optic nerve compression. Radiology. 1996;200(1):123-7.
18. Feldon SE, Lee CP, Muramatsu SK, Weiner JM. Quantitative computed tomography of Graves' ophthalmopathy. Extraocular muscle and orbital fat in development of optic neuropathy. Arch Ophthalmol. 1985;103(2):213-5.
19. Forbes G, Gorman CA, Brennan MD, Gehring DG, Ilstrup DM, Earnest Ft. Ophthalmopathy of Graves' disease: computerized volume measurements of the orbital fat and muscle. AJNR Am J Neuroradiol. 1986;7(4):651-6.
20. Chapman VM, Grottkau BE, Albright M, Salamipour H, Jaramillo D. Multidetector computed tomography of pediatric lateral condylar fractures. J Comput Assist Tomogr. 2005;29(6):842-6, http://dx.doi.org/10.1097/01.rct.0000175504.64707.e3.
21. Bartley GB, Gorman CA. Diagnostic criteria for Graves' ophthalmopathy. Am J Ophthalmol. 1995;119(6):792-5.
22. Wall M, Neahring RK, Woodward KR. Sensitivity and specificity of frequency doubling perimetry in neuro-ophthalmic disorders: a comparison with conventional automated perimetry. Invest Ophthalmol Vis Sci. 2002;43(4):1277-83.
23. Kazim M, Trokel SL, Acaroglu G, Elliott A. Reversal of dysthyroid optic neuropathy following orbital fat decompression. Br J Ophthalmol. 2000;84(6):600-5, http://dx.doi.org/10.1136/bjo.84.6.600.
24. Kennerdell JS, Rosenbaum AE, El-Hoshy MH. Apical optic nerve compression of dysthyroid optic neuropathy on computed tomography. Arch Ophthalmol. 1981;99(5):807-9, http://dx.doi.org/10.1001/archopht.1981.03930010807002.
25. Hallin ES, Feldon SE. Graves' ophthalmopathy: I. Simple CT estimates of extraocular muscle volume. Br J Ophthalmol. 1988;72(9):674-7, http://dx.doi.org/10.1136/bjo.72.9.674.
26. Hudson HL, Levin L, Feldon SE. Graves exophthalmos unrelated to extraocular muscle enlargement. Superior rectus muscle inflammation may induce venous obstruction. Ophthalmology. 1991;98(10):1495-9.
27. Gorman CA. Radiotherapy for Graves' ophthalmopathy: results at one year. Thyroid. 2002;12(3):251-5, http://dx.doi.org/10.1089/105072502753600232.
28. Hu WD, Annunziata CC, Chokthaweesak W, Korn BS, Levi L, Granet DB, et al. Radiographic analysis of extraocular muscle volumetric changes in thyroid-related orbitopathy following orbital decompression. Ophthal Plast Reconstr Surg. 2010;26(1):1-6, http://dx.doi.org/10.1097/IOP.0b013e3181b80fae.
29. Alsuhaibani AH, Carter KD, Policeni B, Nerad JA. Orbital volume and eye position changes after balanced orbital decompression. Ophthal Plast Reconstr Surg. 2011;27(3):158-63.
30. Liao SL, Huang SW. Correlation of retrobulbar volume change with resected orbital fat volume and proptosis reduction after fatty decompression for Graves ophthalmopathy. Am J Ophthalmol. 2011;151(3):465-9 e1, http://dx.doi.org/10.1016/j.ajo.2010.08.042.
31. Regensburg NI, Wiersinga WM, Berendschot TT, Saeed P, Mourits MP. Effect of smoking on orbital fat and muscle volume in Graves' orbitopathy. Thyroid. 2011;21(2):177-81, http://dx.doi.org/10.1089/thy.2010.0218.
32. Bijlsma WR, Mourits MP. Radiologic measurement of extraocular muscle volumes in patients with Graves' orbitopathy: a review and guideline. Orbit. 2006;25(2):83-91, http://dx.doi.org/10.1080/01676830600675319.